

EEG-Based Fractal Analysis of Different Motor Imagery Tasks using Critical Exponent Method

Montri Phothisonthai and Masahiro Nakagawa

Abstract—The objective of this paper is to characterize the spontaneous electroencephalogram (EEG) signals of four different motor imagery tasks and to show hereby a possible solution for the present binary communication between the brain and a machine or a brain-computer interface (BCI). The processing technique used in this paper was the fractal analysis evaluated by the critical exponent method (CEM). The EEG signal was registered in 5 healthy subjects, sampling 15 measuring channels at 1024 Hz.

Each channel was preprocessed by the Laplacian space filtering so as to reduce the space blur and therefore increase the space resolution. The EEG of each channel was segmented and its fractal dimension (FD) calculated. The FD was evaluated in the time interval corresponding to the motor imagery and averaged out for all the subjects (each channel). In order to characterize the FD distribution, the linear regression curves of FD over the electrodes position were applied. The differences FD between the proposed mental tasks are quantified and evaluated for each experimental subject. The obtained results of the proposed method are a substantial fractal dimension in the EEG signal of motor imagery tasks and can be considerably utilized as the multiple-states BCI applications.

Keywords—electroencephalogram (EEG), motor imagery tasks, mental tasks, biomedical signals processing, human-machine interface, fractal analysis, critical exponent method (CEM).

I. INTRODUCTION

AN electroencephalogram (EEG) signal is generated from the natural currents of the billion nerve cells in a human brain. The EEG signals are very helpful information for a novel interfacing technology between a human and a machine such as a brain-computer interface (BCI) [1]. The EEG signals are measuring at the scalp surface through the electrodes or called a noninvasive method. This channel has been providing not only healthy peoples but also patients who are suffering from severe motor impairments and numerous other diseases that they cannot use any of the traditional methods but being cognitive intact [2]. The imagination of motor movement for real applications system can be realized by training the users (or subjects) to control his/her brainwaves. There are many researches proposed the EEG signals of motor imagery tasks for helpful applications such as a robot control [3], a virtual keyboard [4], an assistive appliance [5], and etc. However, the most of previous works based on a binary command since the imagination of left and right hand movement are mostly popular tasks.

There are several theoretical-practical studies on the amount of mental states might be used by a BCI system. However the

The authors are with the Chaos and Fractals Informatics Laboratory (NLAB), Department of Electrical Engineering, Faculty of Engineering, Nagaoka University of Technology, 1603-1 Kamitomioka, Nagaoka, Niigata 940-2188 Japan.

TEL: +81-2-5847-1611 (ext. 5146) FAX: +81-258-47-9500

most relevant issue is that the mental tasks could be clearly differences [6]. At present, the advances in the research of BCI systems aims to improve the information transference rate (ITR) and a useful alternative is to implement multi-states systems.

The event-related desynchronization (ERD) and synchronization (ERS) or ERD/ERS patterns are widely used to reveal the natural phenomenal responses in EEG signal of imaging. There are several methods have been proposed to detect the ERD/ERS. The method based on a power spectral density (PSD) [7]. This technique has always been a popular method for frequency-based extracting and classifying EEG signals. However, the power spectrum was not able to extracts the distinguishing features. The C3 and C4 electrode signals were utilized for extraction of the autoregressive (AR) coefficients [8] and multivariate autoregressive (MVAR) model [9]. The feature vector consisting of these coefficients was used for classification. However, the results reveal that the method is not suitable as features for the data set used because the majority of AR analysis assumes the input data is linear and stationary and to be zero mean. In [10]–[11], proposed a time-frequency analysis of EEG signals and in [12] proposed the new imagery tasks so that the imagination of yes/no as the mental tasks. This technique assists the subjects not require any of training. Next, the use of fractal dimension (FD) applied to EEG signals and proposed to BCI systems have been previously suggested by other papers [13]–[15]. However, those methods are applicable of using for only the applications of binary command. For the recent reports, C. Neupera and et al. [16] and G. Pfurtscheller and et al. [17], presented the possible significant of the kind of imagery such as kinesthetic motor imagery, visual motor imagery, different motor imagery, etc. They proposed the EEG single-trial classification the imagery of different motor imagery tasks. The linear classification with electrode position at C3 and C4 were placed on a sensorimotor area. This method shows the ERD/ERS response according to the imaginary of tasks. However, the method based on two electrodes position it is not sufficient to reveal the hidden information of mental tasks.

In this paper, we propose a possible improvement for the problem of binary communication by increasing the number of mental tasks up to four, however, so that we may affirm that the processing method is applicable to multi-states BCI systems, the differences between the proposed mental tasks should be quantified and evaluated for each experimental subject. The mental tasks proposed in this paper have not been previously analyzed through fractal techniques, the analysis of the mental tasks proposed through the fractal analysis.

The paper proceeds as follows. Section 2 the proposed method is presented. And the experimental results in Sect. 3, discussed in Sect. 4. Finally, the paper is concluded in Sect. 5.

II. METHODS

A. EEG signals acquisition and experimental paradigm

The electrodes were placed according to the 10-20 international system as depicted in Fig. 1.

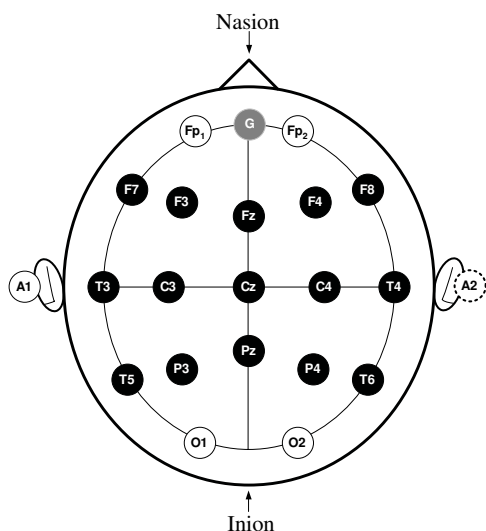


Fig. 1. The electrode positions of 12 channels were placed on the scalp for EEG signal acquisition is marked in black circles. The grounding electrode is marked in gray circle and the referencing electrode is marked in dotted circle.

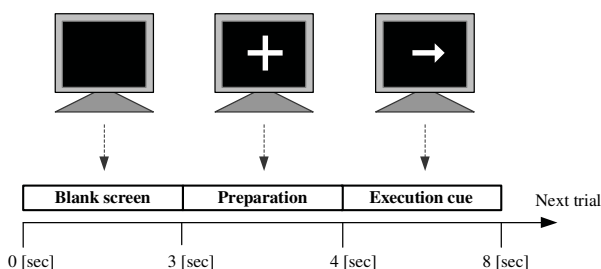


Fig. 2. One-trial epoch for time sequence of the experiment with the indicators on a monitor.

In the experiment we use a multiple channel amplifier (MEG-6116; Nihon Kohden, Tokyo, Japan), analog-to-digital converter (PC-CARD-DAS16/16; Measurement Computing, MA, USA), and the EEG electrode paste (Z-401CE; Nihon Kohden, Tokyo, Japan) is used for impedance reducing. The EEG signals were digitized at 1024 samples/sec; resolution 16 bits/sample; and signals were analog bandpass filtered between 1.5 and 100 Hz. We have used the notch filter to protect the artifacts at 50 Hz cut-off. The experimental paradigm we have tested with three males (M1, M2, and M3) and two females (F1 and F2). Their age between 21-32 years old (mean age 26.8 years, SD 4.3); we collect the 80-trials data per subject (20-trials/mental task). They sat in a comfortable chair in an electrically shielded room and watching a 15" monitor from a distance of about 1.0 meter. Four mental tasks

were given subjects perform they consist of 1) Imagine to left finger-index movement; 2) Imagine to right finger-index movement; 3) Imagine to tongue movement; and 4) Imagine to feet movement.

We set the one-trial epoch of time period is 8 seconds throughout the experiment as depicted in Fig. 2 also the time period of experiment was divided into three periods. First period, the subjects have to relax with eyes-opened which this period is represented by the blank screen. Second period, the subjects are preparing to perform the tasks which this period the cross is displayed. Third period, the subjects perform the tasks with eyes-opened which this period is represented by the indicators. To indicate which tasks will be perform, we have use the several kinds of indicator as the left arrow for left finger-index movement, the right arrow for right finger-index movement, the down arrow for feet movement, and the dash sign for tongue movement.

B. Preprocessing

Firstly, the raw EEG signals were recorded from the subjects should prepare to preprocessing. For preprocessing that EEG patterns can be detected with surface Laplacian (SL) filtering than with the unprocessed raw potentials [18]. The SL filtering reduces considerably the spatial blur of the recorded EEG signals due to the head as a volume conductor. In addition, the recorded EEG signals require the evaluation of the second order spatial derivative of the scalp surface potential that is an estimation of the radial neural current density following through the human skull towards the cortex. The SL filtering of a potential field can be calculated by using two dimensional second derivative operator is given by:

$$L_s = -\nabla^2 \phi_{xy} = -\left\{ \frac{\partial^2 \phi}{\partial x^2} + \frac{\partial^2 \phi}{\partial y^2} \right\}, \quad (1)$$

where ϕ is a function of a three dimensional space, x, y, z , in case of scalp potential. Since the distances of the nearest electrodes are small in relation to the curvature of the head, a planar geometry, ϕ_{xy} , can be assumed as a good approximation of the local surface. In practice, the SL filtering at the electrode can be numerically estimated by the weighted summation of potentials at the electrode and its nearest neighboring surround by Hjorth's method [19]. In this paper we have modified the SL filtering that appropriated with the electrode positions as follows:

$$\hat{x}_i = x_i - \frac{1}{M} \sum_{j \in N_i} x_j, \quad (2)$$

where \hat{x}_i is the output signals from SL filtering, x_i is the raw EEG signals at i -th channel, N_i is an index set of the neighboring channels, and M is the constant values where $M = 2$ if the current channels are F7, F8, T5, and T6, and $M = 3$ if the current channels are F2, F3, Fz, T3, T4, P3, P4, and Pz, and otherwise $M = 4$.

C. Fractal evaluation based on critical exponent method

The fractal concept has been widely used to describe the objects in space since it has been found to be useful for

analysis of biological signals [20][21]. The time series with fractal nature to be describable by the functions of fractional Brownian motion (fBm), for which the fractal dimensions can easily be set. The fBm with Hurst function, H , has been described in [22]. This paper proposed the fractal dimension evaluation based on the critical exponent method (CEM) [23]. The power spectral density (PSD), $P_H(\nu)$, of observed signals in the frequency domain is determined as:

$$P_H(\nu) \sim \nu^{2H+1} = \nu^{-\beta}, \quad (3)$$

In the CEM, the moment I_α of the PSD is determined as:

$$I_\alpha = \int P_H(\nu) \nu^\alpha d\nu, \quad (-\infty < \alpha < \infty), \quad (4)$$

We will consider the limited frequency bands and substitute Eq. (3) in Eq. (4) thus the equation was given as:

$$I_\alpha \sim \int_1^\Omega \nu^{\alpha-\beta} d\nu = \frac{1}{\alpha-\beta+1} (\Omega^{\alpha-\beta+1} - 1), \quad (5)$$

$$= \frac{2}{U} \exp\left(\frac{U \log \Omega}{2}\right), \quad (6)$$

where α is the moment exponent, Ω is the frequency variable which was normalized to the lower bound of the integration region as 1, and let $U = \alpha - \beta + 1$. In the CEM, the condition of $U = 0$ is satisfied for the moment of critical exponent as $\alpha = \alpha_c$ at which the value of the third order derivative of $\log I_\alpha$ with respect to is zero as the following equation:

$$\frac{d^3 \log I_\alpha}{d\alpha^3} = \frac{I_\alpha'''' I_\alpha^2 - 3 I_\alpha'' I_\alpha' I_\alpha + 2 (I_\alpha')^3}{I_\alpha^3}, \quad (7)$$

Finally, from this value of α_c , $\beta = \alpha_c - 1$ and the estimated fractal dimension is given as:

$$D = 2 - \frac{\alpha_c}{2}. \quad (8)$$

where α_c is the critical exponent value. Figure 3 shows the determination of the critical exponent value of the traditional fBm signal with $H = 0.07$ (or $D = 1.930$) and the sample length is 1,024 points. The CEM can evaluate its fractal dimension was $D = 1.9320$.

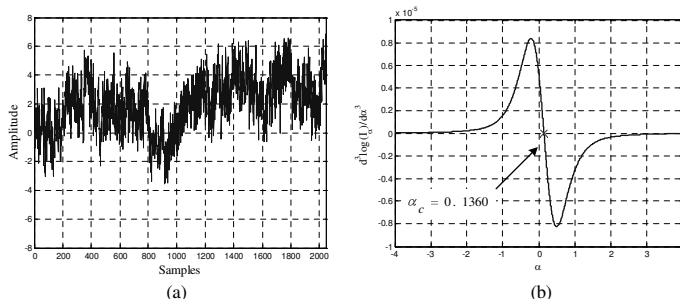


Fig. 3. Determination method of the critical exponent value. (a) Traditional fBm signal with $H = 0.07$. (b) Third order derivative of the logarithmic function and the zero crossing point.

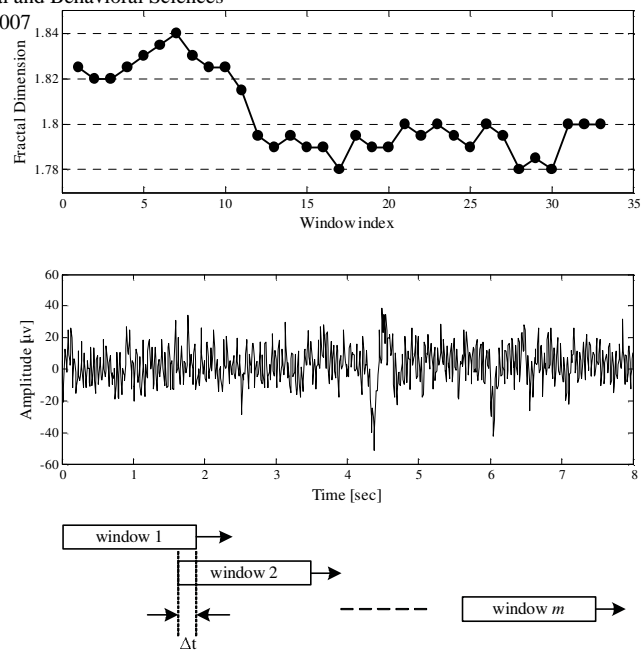


Fig. 4. Typical example of the SL filtered EEG signals and its fractal dimension over time. The fractal dimension was estimated based on CEM with TDFD.

D. Time-dependent fractal dimension

The EEG data contain the fluctuations concerned with frequency, amplitude, self-affine property, chaotic behavior, etc. Therefore, if we divide the whole time-sequential data into several short time intervals and measure the degrees of freedom of the fluctuations inside these time-intervals, we can observe the change in the degree of fluctuations with respect to time. These fluctuations are effectively characterized by the fractal dimensions. In this paper, we will approach the CEM in order to evaluate the fraction dimensions and called the time-dependent fractal dimension (TDFD). In practice, we will divide the EEG data that obtained from the SL filtering into short time intervals by a windowing with a window function. We then evaluate the fractal dimensions of the points inside this windowing. Next, we move this window by n points (Δt) and again evaluate the fractal dimension of moved window. By repeating this process throughout the whole EEG data, we can observe the change in the fractal dimension with respect to time. In the case of TDFD, the horizontal axis is the window index and vertical axis is the fractal dimension value. Figure 3 shows a typical example of the EEG signal and its fractal dimension through the experiment.

III. EXPERIMENTAL RESULTS

We set up the acting stimuli in the experiment due to help subject can easily imagines the desired tasks. The acting stimuli for each of tasks shown as follows:

- 1) Feet movement: imagine to left-right moving.
- 2) Left finger-index movement: imagine to repeating mouse click by using left finger-index of left hand side.
- 3) Right finger-index movement: imagine to repeating mouse click by using right finger-index of right hand side.

TABLE I
THE AVERAGE VALUES OF FRACTAL DIMENSIONS AT EACH TASKS FROM
SUBJECT SM1.

| Channel | FT-MI | LF-MI | RF-MI | TG-MI |
|---------------|---------|---------|---------|---------|
| F7 | 1.7550 | 1.7425 | 1.7528 | 1.7519 |
| F3 | 1.8053 | 1.7381 | 1.7613 | 1.7966 |
| Fz | 1.8356 | 1.7541 | 1.8062 | 1.7731 |
| F4 | 1.7891 | 1.705 | 1.7247 | 1.795 |
| F8 | 1.9444 | 1.7975 | 1.8622 | 1.9038 |
| T3 | 1.8606 | 1.7478 | 1.7925 | 1.8062 |
| C3 | 1.8519 | 1.7634 | 1.8181 | 1.7659 |
| Cz | 1.7953 | 1.7394 | 1.7997 | 1.7559 |
| C4 | 1.8550 | 1.7506 | 1.785 | 1.7641 |
| T4 | 1.9194 | 1.8122 | 1.7875 | 1.8463 |
| T5 | 1.8525 | 1.8147 | 1.7931 | 1.8091 |
| P3 | 1.7866 | 1.7594 | 1.7297 | 1.7469 |
| Pz | 1.8259 | 1.7469 | 1.7888 | 1.7369 |
| P4 | 1.7931 | 1.7241 | 1.7438 | 1.7203 |
| T6 | 1.8816 | 1.8716 | 1.8303 | 1.8700 |
| Averaged S.D. | ±0.0116 | ±0.0102 | ±0.0153 | ±0.0104 |

TABLE II

THE AVERAGE VALUES OF FRACTAL DIMENSIONS AT EACH TASKS FROM
SUBJECT SM2.

| Channel | FT-MI | LF-MI | RF-MI | TG-MI |
|---------------|---------|---------|---------|---------|
| F7 | 1.7869 | 1.6906 | 1.7147 | 1.7437 |
| F3 | 1.8338 | 1.7044 | 1.7163 | 1.8131 |
| Fz | 1.8863 | 1.7159 | 1.7569 | 1.8053 |
| F4 | 1.8025 | 1.6747 | 1.6984 | 1.765 |
| F8 | 1.9647 | 1.7766 | 1.7328 | 1.8266 |
| T3 | 1.8791 | 1.7672 | 1.765 | 1.8569 |
| C3 | 1.8909 | 1.7663 | 1.7622 | 1.8547 |
| Cz | 1.8556 | 1.7097 | 1.7528 | 1.8078 |
| C4 | 1.9056 | 1.7334 | 1.7284 | 1.7878 |
| T4 | 1.8728 | 1.7766 | 1.7769 | 1.8438 |
| T5 | 1.9372 | 1.8038 | 1.7759 | 1.8641 |
| P3 | 1.8203 | 1.7112 | 1.7306 | 1.7647 |
| Pz | 1.9075 | 1.7541 | 1.7316 | 1.7987 |
| P4 | 1.8053 | 1.6981 | 1.7019 | 1.7253 |
| T6 | 1.9206 | 1.8322 | 1.8228 | 1.8584 |
| Averaged S.D. | ±0.0108 | ±0.0110 | ±0.0124 | ±0.0102 |

4) Tongue movement: imagine up-down moving.

In the experiment, the EEG signals during imagined movement (4 sec to 8 sec) in each of trial were processed (or 4,096 points.) To evaluate the fractal dimensions respect to TDFD, we set a window function is a rectangular type, window size = 1,024 points (1 s), moving window with intervals = 128 points (62.5 ms).

Therefore, the time resolution to evaluating of the fractal dimension was 62.5 ms. The number of obtained points can determine from $N_{FD} = [(L - L_w)/\Delta t] + 1$ where L is a sample length of observed EEG data, L_w is a window length, and Δt is an interval. Thus we will obtain 25 points of fractal dimension values per channel over the imagination period. The each of windowed segments were evaluated in frequency domain through the L_w -points fast Fourier transforms (FFT) to determine the critical exponent value of the CEM as defined in Eq. 7. Next, the abbreviations will be used for convenient representation throughout the section as follows: imagination of feet movement (FT-MI); imagination of left finger-index movement (LF-MI); imagination of right finger-index movement (RF-MI); and imagination of tongue movement (TG-MI).

TABLE III

THE AVERAGE VALUES OF FRACTAL DIMENSIONS AT EACH TASKS FROM
SUBJECT SM3.

| Channel | FT-MI | LF-MI | RF-MI | TG-MI |
|---------------|---------|---------|---------|---------|
| F7 | 1.7709 | 1.7212 | 1.7078 | 1.7281 |
| F3 | 1.8225 | 1.8091 | 1.7131 | 1.8006 |
| Fz | 1.8503 | 1.8653 | 1.7322 | 1.7397 |
| F4 | 1.7897 | 1.8103 | 1.6747 | 1.7941 |
| F8 | 1.9300 | 1.8047 | 1.7706 | 1.8381 |
| T3 | 1.8381 | 1.8331 | 1.7631 | 1.8369 |
| C3 | 1.8478 | 1.8597 | 1.745 | 1.8116 |
| Cz | 1.8213 | 1.7963 | 1.7288 | 1.7209 |
| C4 | 1.835 | 1.8266 | 1.7441 | 1.7222 |
| T4 | 1.9431 | 1.8194 | 1.7762 | 1.9344 |
| T5 | 1.8719 | 1.9303 | 1.7669 | 1.8344 |
| P3 | 1.8000 | 1.7806 | 1.7031 | 1.9109 |
| Pz | 1.8219 | 1.7697 | 1.7209 | 1.8131 |
| P4 | 1.7978 | 1.7144 | 1.7294 | 1.6950 |
| T6 | 1.8734 | 1.9119 | 1.7938 | 1.8406 |
| Averaged S.D. | ±0.0125 | ±0.0132 | ±0.0121 | ±0.0144 |

TABLE IV

THE AVERAGE VALUES OF FRACTAL DIMENSIONS AT EACH TASKS FROM
SUBJECT SF1.

| Channel | FT-MI | LF-MI | RF-MI | TG-MI |
|---------------|---------|---------|---------|---------|
| F7 | 1.7178 | 1.6934 | 1.7503 | 1.6331 |
| F3 | 1.7122 | 1.8019 | 1.8122 | 1.6231 |
| Fz | 1.7441 | 1.7644 | 1.7959 | 1.6584 |
| F4 | 1.7022 | 1.8119 | 1.7806 | 1.6347 |
| F8 | 1.7919 | 1.8641 | 1.8331 | 1.7034 |
| T3 | 1.8106 | 1.8213 | 1.8056 | 1.7597 |
| C3 | 1.7775 | 1.7481 | 1.7625 | 1.7378 |
| Cz | 1.7769 | 1.6994 | 1.7381 | 1.7147 |
| C4 | 1.8000 | 1.7112 | 1.7428 | 1.7206 |
| T4 | 1.7875 | 1.8600 | 1.8119 | 1.7797 |
| T5 | 1.8341 | 1.8091 | 1.7819 | 1.8756 |
| P3 | 1.7625 | 1.7503 | 1.7072 | 1.7953 |
| Pz | 1.7628 | 1.7222 | 1.7025 | 1.8044 |
| P4 | 1.7741 | 1.6797 | 1.7412 | 1.7403 |
| T6 | 1.8438 | 1.8809 | 1.8347 | 1.9144 |
| Averaged S.D. | ±0.0112 | ±0.0131 | ±0.0107 | ±0.0105 |

TABLE V

THE AVERAGE VALUES OF FRACTAL DIMENSIONS AT EACH TASKS FROM
SUBJECT SF2.

| Channel | FT-MI | LF-MI | RF-MI | TG-MI |
|---------------|---------|---------|---------|---------|
| F7 | 1.7381 | 1.6609 | 1.6866 | 1.715 |
| F3 | 1.8016 | 1.6841 | 1.6612 | 1.8719 |
| Fz | 1.8319 | 1.7234 | 1.7294 | 1.8441 |
| F4 | 1.7672 | 1.6528 | 1.6781 | 1.8059 |
| F8 | 1.8634 | 1.715 | 1.7916 | 1.8781 |
| T3 | 1.8394 | 1.7416 | 1.7594 | 1.8856 |
| C3 | 1.8172 | 1.7572 | 1.7197 | 1.9591 |
| Cz | 1.8113 | 1.7569 | 1.7072 | 1.8322 |
| C4 | 1.8091 | 1.7113 | 1.7528 | 1.8522 |
| T4 | 1.7903 | 1.7466 | 1.8166 | 1.8872 |
| T5 | 1.8606 | 1.7934 | 1.7988 | 1.9863 |
| P3 | 1.8225 | 1.7488 | 1.7450 | 1.8419 |
| Pz | 1.7581 | 1.7653 | 1.7216 | 1.8334 |
| P4 | 1.7369 | 1.6869 | 1.6988 | 1.7716 |
| T6 | 1.8806 | 1.7791 | 1.8444 | 1.9894 |
| Averaged S.D. | ±0.0147 | ±0.0124 | ±0.0113 | ±0.0128 |

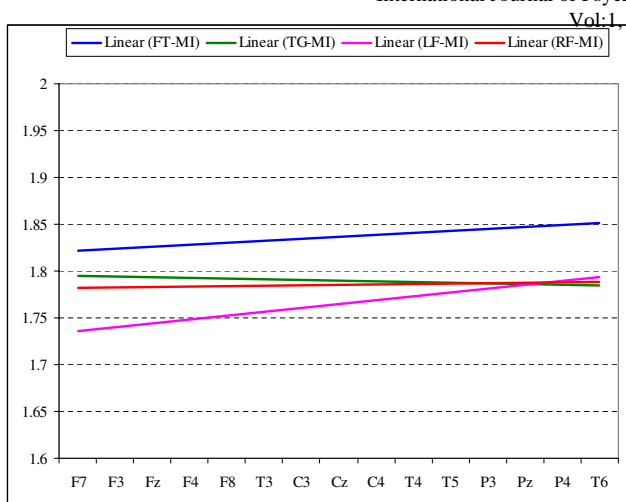


Fig. 5. Linear regression curves of the four motor imagery tasks over the electrodes position, subject SM1.

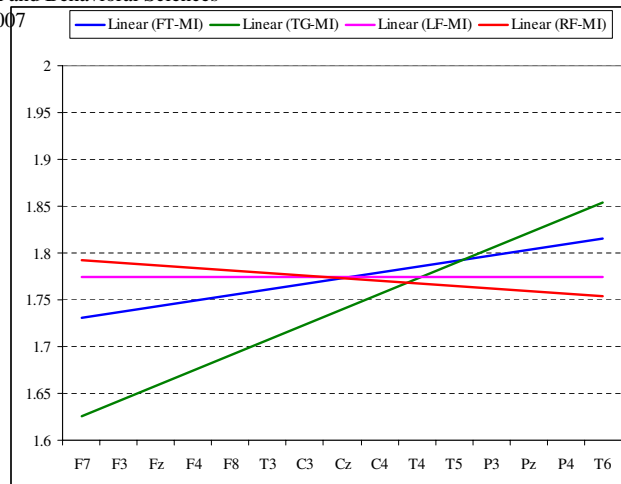


Fig. 8. Linear regression curves of the four motor imagery tasks over the electrodes position, subject SF1.

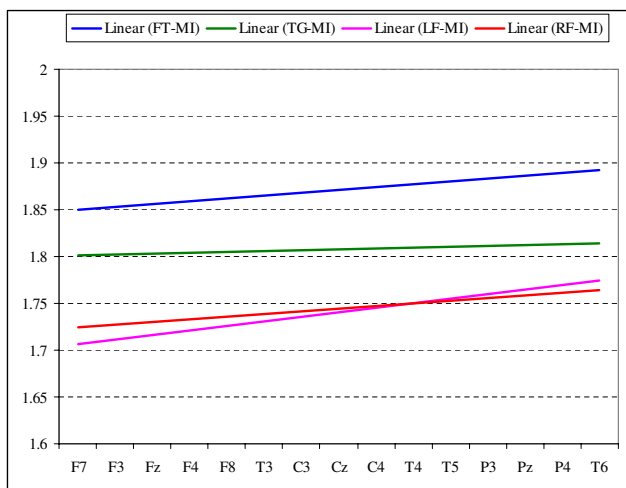


Fig. 6. Linear regression curves of the four motor imagery tasks over the electrodes position, subject SM2.

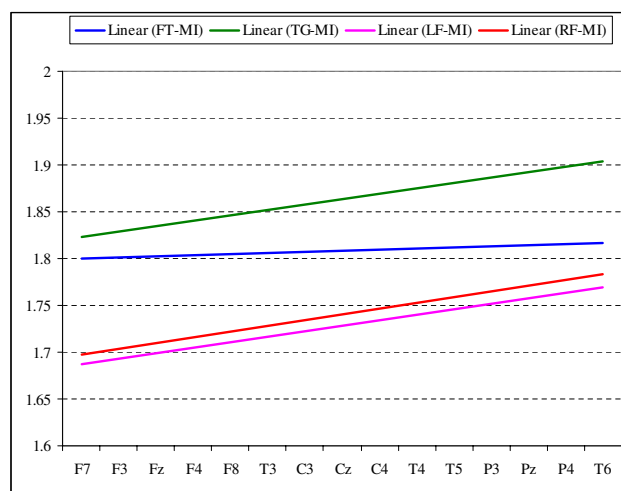


Fig. 9. Linear regression curves of the four motor imagery tasks over the electrodes position, subject SF2.

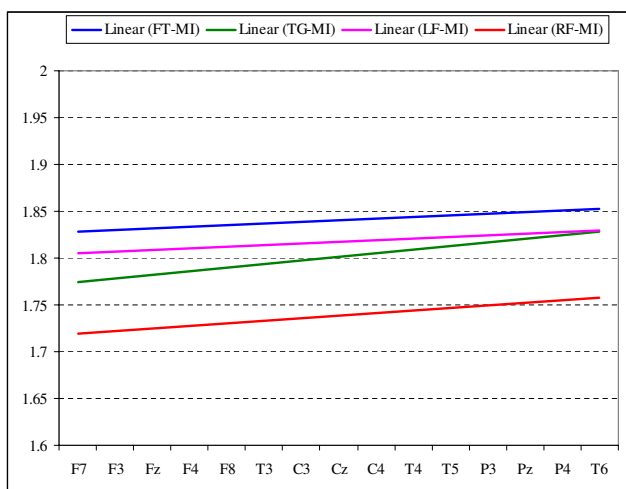


Fig. 7. Linear regression curves of the four motor imagery tasks over the electrodes position, subject SM3.

At the experimental paradigm the fractal dimension during imagination of motor movement was evaluated (4 to 8 s) thus the TDFD at all 25 points were also evaluated. The reason is that, its fractal dimensions can reveal the patterns change according to the complexity of natural EEG signal property. The average values of fractal dimension and standard deviation of each channel from all subjects are shown as Table I. to Table V. Since each subject will present different EEG patterns during the motor imagery tasks. As it is mentioned by Curran et al [24], the strategies used to produce a determined motor imagery are show separately, therefore the FD characteristics of the EEG will be different. To present it, the linear regression curves were applied as shown in Fig. 5 to Fig. 9.

IV. DISCUSSIONS

As the obtained results, in Fig. 5 to Fig.9, the subject SM1 shows that the most of FD distribution of FT-MI higher than other mental tasks over whole positions. Moreover, in this study shows that the trend of FD during FT-MI of the

participated three males (SM1, SM2, and SM3) produce higher than other mental tasks since the FD was about 1.8 to 1.9. For the subject SF1 as shown in Fig. 8 produced the high FD at only on the central area of the brain (Cz, C4, and T4). The subject SF2 show the FD of FT-MI lowers than only TG-MI.

For the FD of LF-MI and RF-MI their linear regression curves are closely same shape. However, we can determine the different FD characteristics by the areas such as the frontal area (F7, F3, Fz, F4, and F8) of all subjects produces the FD of RF-MI higher than LF-MI since the range FD minimum at 1.69 to maximum at 1.84.

And for the FD of TG-MI higher than other metal tasks only subject SF2. Since the three males produced the FD of TG-MI was about 1.8 and always lower than the FD of FT-MI all over area of the brain. The subject SF1 shows the FD lower than other mental tasks at the frontal and central areas.

The fractal dimension evaluation based on CEM is proposed to be useful information for the analysis of time dependence of data in which the fractal dimension changes in imagined EEG signals. Since in the human brain is a highly complex nonlinear system which shows chaotic dynamics. The human EEG possesses a self-affine property with a fractional dimension corresponding to a chaotic behavior of the neurons that time series have a fractal or multifractal temporal structure [12], [21]. A higher fractal dimension indicates a more complicated structure of EEG signals, or the quantity of information embodied in a pattern. Moreover, there is the evident of fractal dimension of mental tasks as imagined movements were existed.

V. CONCLUSIONS

The fractal analysis of EEG signals of different motor imagery tasks has been proposed. We evaluated its fractal dimension based on CEM with TDFD. The critical exponent value, which is determined by CEM, characterizes the self-affine property of the EEG signal and had direct relation to the electrodes position. Therefore, the fractal dimensions were effective for classifying the motor imagery tasks. The obtained result of the proposed method is a substantial fractal dimension in the EEG signal of motor imagery tasks. Moreover, the method described in this paper can be considerably utilized both the EEG-based classifications and the multiple-commands in the BCI applications.

ACKNOWLEDGMENT

This research was partially supported in part by the 21st Century COE (Center of Excellence) Program "Global Renaissance by Green Energy Revolution" and the Grant-in-Aid for Scientific Research (15300070) from the Ministry of Education, Culture, Sports, Science and Technology of Japan. The authors would like to thank the subjects who took part in this research.

REFERENCES

[1] S. G. Mason and G. E. Birch, "A general framework for brain-computer interface design", *IEEE Trans. Neural Net. Syst. Rehab. Eng.*, vol. 11, pp. 70–85, 2003.

[2] J. R. Wolpaw, N. Birbaumer, D. J. McFarland, G. Pfurtscheller, and T. M. Vaughan, "Brain-computer interface for communication and control", *Clin. Neurophysiol.*, vol. 113, pp. 767–791, 2002.

[3] J. R. Millan, F. Renkens, J. Mourino, and W. Gerstner, "Noninvasive brain-actuated control of a mobile robot by human EEG". *IEEE Trans. Biome. Eng.*, vol. 51, pp. 1026–1033, 2004.

[4] B. Obermaier, G. R. Muller, and G. Pfurtscheller, "Virtual keyboard controlled by spontaneous EEG activity", *IEEE Trans. Neural Net. Syst. and Rehab. Eng.*, vol. 11, pp. 422–426, 2003.

[5] P. R. Kennedy, R. A. Bakay, M. M. Moore, K. Adams, and J. Goldwaithe, "Direct control of a computer from the human central nervous system", *IEEE Trans. Rehab. Eng.*, vol. 8, pp. 198–202, 2000.

[6] G. Dornhege, B. Blankertz, G. Curio, and K. Muller, "Boosting Bit Rates in Noninvasive EEG Single-Trial Classifications by Feature Combination and Multiclass Paradigms", *IEEE Transactions On Biomedical Engineering*, vol. 51, pp. 993–1002, 2004.

[7] J. R. Millan, F. Renkens, J. Mourino, and W. Gerstner, "Brain-actuated interaction", *Artif. Intell.*, vol. 159(1–2), pp. 241–259, 2004.

[8] G. Pfurtscheller, C. Neuper, A. Schlogl, K. Lugger, "Separability of EEG signals recorded during right and left motor imagery using adaptive autoregressive parameters", *IEEE Trans. Rehab. Eng.*, vol. 6, pp. 316–325, 1998.

[9] C. W. Anderson, E. A. Stolz, S. Shamsunder, "Multivariate autoregressive models for classification of spontaneous electroencephalogram during metal tasks", *IEEE Trans. Biomed. Eng.*, vol. 45, pp. 277–286, 1998.

[10] T. Wang, J. Deng, and B. He, "Classifying EEG-based motor imagery tasks by means of time-frequency synthesized spatial patterns", *Clinical Neurophysiol.*, vol. 115, pp. 2744–2753, 2004.

[11] L. Qin, L. Ding, and B. He, "Motor imagery classification by means of source analysis for brain-computer interface applications", *J. Neural Eng.*, vol. 1, pp. 135–141, 2004.

[12] M. Phothisonothai and M. Nakagawa, "EEG-based classification of new imagery tasks using three-layer feedforward neural network classifier for brain-computer interface", *J. Phys. Soc. Jpn.*, vol. 75, pp. 104801–1–104801–6, 2006.

[13] R. Boostani and M. E. Moradi, "A new approach in the BCI research based on fractal dimension as feature and Adaboost as classifier", *J. Neural Eng.*, vol. 1, pp. 212–217, 2004.

[14] A. Bashashati, R.K. Ward, G.E. Birch, M.R. Hashemi, and MA. Khalilzadeh, "Fractal Dimension-Based EEG Biofeedback System", *Proc. of the 25 Annual Inter. Conf. of the IEEE EMBS Cancun*, vol. 3, pp. 17–21, 2003.

[15] H. Prei, W. Lutzenberger, F. Pulvermuller, and N. Birbaumer, "Fractal dimensions of short EEG time series in humans", *Neuroscience Letters* vol. 225, pp. 77–80, 1997.

[16] C. Neupera, R. Scherer, M. Reinerd, G. Pfurtscheller, "Imagery of motor actions: differential effects of kinesthetic and visual-motor mode of imagery in single-trial EEG", *Cognitive Brain Research*, vol. 25, pp. 668–677, 2005.

[17] G. Pfurtscheller, C. Brunner, A. Schlogl, "Lopes da Silvab FH. Mu rhythm (de)synchronization and EEG single-trial classification of different motor imagery tasks", *NeuroImage*, vol. 31, pp. 153–159, 2006.

[18] D. J. McFarland, L. M. McCane, S. V. David, J. R. Wolpaw, "Spatial filter selection for EEG-based communication", *Electroenceph. Clin. Neurophysiol.*, vol. 103, pp. 386–394, 1997.

[19] B. Hjorth, "An on-line transformation of EEG scalp potentials into orthogonal source derivations", *Electroenceph. Clin. Neurophysiol.*, vol. 39, pp. 526–530, 1975.

[20] M. Akay and E. J. H. Mulder, "Effects of maternal alcohol intake on fractal properties in human fetal breathing dynamics", *IEEE Trans. Biomed. Eng.*, vol. 45, pp. 1097–1103, 1998.

[21] J. Gnitecki and Z. Moussavi, "The fractality of lung sounds: a comparison of three waveform fractal dimension algorithms", *Chaos, Solitons and Fractals*, vol. 26, pp. 1065–1072, 2005.

[22] M. Nakagawa, *Chaos and fractals in engineering*, World Scientific, Singapore, pp. 1–41, 1999.

[23] M. Nakagawa, "A critical exponent method to evaluate fractal dimension of self-affine data", *J. Phys. Soc. Jpn.*, vol. 62, pp. 4233–4239, 1993.

[24] E. Curran and M. Stokes, "Learning to control brain activity: A review of the production and control of EEG components for driving brain-computer interface (BCI) systems", *Brain and Cognition*, vol. 51, pp. 326–336, 2003.